

# Alterations in inorganic phosphate in mouse hindlimb muscles during limb disuse<sup>†</sup>

Neeti Pathare,<sup>1</sup> Krista Vandendorpe,<sup>1</sup> Min Liu,<sup>1</sup> Jennifer E. Stevens,<sup>1,2</sup> Ye Li,<sup>1</sup> Tiffany N. Frimel<sup>1</sup> and Glenn A. Walter<sup>3\*</sup>

<sup>1</sup>Department of Physical Therapy, University of Florida, Gainesville, FL, USA

<sup>2</sup>Malcom Randall VA Medical Center, VA RR&D Brain Rehabilitation Research Center, Gainesville, FL, USA

<sup>3</sup>Department of Physiology and Functional Genomics, University of Florida, Gainesville, FL, USA

Received 8 November 2006; Revised 8 January 2007; Accepted 17 January 2007

**ABSTRACT:** Muscle disuse induces a wide array of structural, biochemical, and neural adaptations in skeletal muscle, which can affect its function. We recently demonstrated in patients with an orthopedic injury that cast immobilization alters the resting  $P_i$  content of skeletal muscle, which may contribute to loss of specific force. The goal of this study was to determine the direct effect of disuse on the basal phosphate content in skeletal muscle in an animal model, avoiding the confounding effects of injury/surgery.  $^{31}\text{P}$  and  $^1\text{H}$  MRS data were acquired from the gastrocnemius muscle of young adult mice (C57BL/6 female,  $n = 8$ ), at rest and during a reversible ischemia experiment, before and after 2 weeks of cast immobilization. Cast immobilization resulted in an increase in resting  $P_i$  content (75%;  $p < 0.001$ ) and the  $P_i$  to phosphocreatine (PCr) ratio ( $P_i/\text{PCr}$ ; 80%,  $p < 0.001$ ). The resting concentrations of ATP, PCr and total creatine (PCr + creatine) and the intracellular pH were not significantly different after immobilization. During ischemia (30 min), PCr concentrations decreased to  $54 \pm 2\%$  and  $52 \pm 6\%$  of the resting values in pre-immobilized and immobilized muscles, respectively, but there were no detectable differences in the rates of  $P_i$  increase or PCr depletion ( $0.55 \pm 0.01 \text{ mM min}^{-1}$  and  $0.52 \pm 0.03 \text{ mM min}^{-1}$  before and after immobilization, respectively;  $p = 0.78$ ). At the end of ischemia, immobilized muscles had a twofold higher phosphorylation potential ( $[\text{ADP}][P_i]/[\text{ATP}]$ ) and intracellular buffering capacity ( $3.38 \pm 0.54$  slykes vs  $6.18 \pm 0.57$  slykes). However, the rate of PCr resynthesis ( $k_{\text{PCr}}$ ) after ischemia, a measure of *in vivo* mitochondrial function, was significantly lower in the immobilized muscles ( $0.31 \pm 0.04 \text{ min}^{-1}$ ) than in pre-immobilized muscles ( $0.43 \pm 0.04 \text{ min}^{-1}$ ). In conclusion, our findings indicate that 2 weeks of cast immobilization, independent of injury-related alterations, leads to a significant increase in the resting  $P_i$  content of mouse skeletal muscle. The increase in  $P_i$  with muscle disuse has a significant effect on the cytosolic phosphorylation potential during transient ischemia and increases the intracellular buffering capacity of skeletal muscle. Copyright © 2007 John Wiley & Sons, Ltd.

**KEYWORDS:** inorganic phosphate; MRS; immobilization; oxidative capacity; skeletal muscle; mouse

## INTRODUCTION

Muscle has a tremendous capacity to adapt to changes in its functional demands, as shown by the desired increases in strength and endurance that accompany exercise and training (1). Muscle also adapts to forced inactivity or disuse, such as occurs during bed rest, microgravity, and limb immobilization (2). Muscle adaptations to disuse are characterized by a loss of muscle mass, muscle weakness,

and a decrease in muscle specific force (force per unit area) (2,3). There is evidence that neural adaptations contribute to the decrement in muscle specific force (4), although it has been postulated that mechanisms distal to the sarcoplasmic reticulum also play a role (5). We recently demonstrated in patients with an orthopedic injury that immobilization in a lower limb cast significantly increases the resting inorganic phosphate ( $P_i$ ) content and suggested that  $P_i$  may contribute to the loss in force production following disuse (6–8). However, in these patients, we could not isolate the effect of cast immobilization from potential deleterious side effects of the injury or surgery. Therefore, this study aims to investigate the effect of cast immobilization on the resting phosphate content of skeletal muscle in an animal model (mouse), circumventing the confounding effect of injury or surgery.

There is substantial evidence from skinned fiber studies that  $P_i$  inhibits muscle force production (9–11). Specifically, it has been demonstrated that  $P_i$  inhibits actomyosin

\*Correspondence to: G. A. Walter, Department of Physiology and Functional Genomics, PO Box 100274, University of Florida, Gainesville, FL 32610, USA.

E-mail: glennw@phys.med.ufl.edu

<sup>†</sup>Preliminary reports of these experiments were presented at the 13<sup>th</sup> Scientific Meeting of the International Society of Magnetic Resonance in Medicine, Miami, 2005.

Grant Support: RO1HD37645, R01HL078670, R01HD42955.

**Abbreviations used:**  $k_{\text{PCr}}$ , phosphocreatine recovery rate constant;  $\text{pH}_i$ , intracellular pH; PCr, phosphocreatine;  $Q_{\text{max}}$ , maximum *in vivo* oxidative ATP synthesis rate; TCr, total creatine;  $V_{\text{meas}}$ , initial rate of PCr resynthesis measured during first 2 min of PCr recovery.

cross-bridge cycling and suppresses muscle force via a shift in the  $\text{Ca}^{2+}$ /force curve (11). Raised concentrations of phosphate are thought to result in a net shift of cross bridges from a strongly bound, high-force-producing state to a weakly bound, low-force-producing state (10). In our previous investigation, we also examined the inhibitory effect of  $\text{P}_i$  on force production in skinned human muscle fibers and demonstrated that varying the  $\text{P}_i$  concentrations within the ranges observed *in vivo* (4–10 mM) reduces force production by ~16% (8). An increase in resting  $\text{P}_i$  content may also have other important functional consequences. A large number of physiological studies have shown that  $\text{P}_i$  plays a regulatory role in mitochondrial oxidative phosphorylation (12–14) and is one of the major buffers involved in the regulation of intracellular pH ( $\text{pH}_i$ ) (15,16).  $^{31}\text{P}$  MRS is commonly used to study *in vivo* oxidative ATP production and  $\text{P}_i$  concentrations and to assess the buffering capacity of skeletal muscle (17,18). Therefore the secondary aim of this study was to monitor the effect of alterations in resting  $\text{P}_i$  content resulting from disuse on the phosphate and  $\text{pH}_i$  kinetics of immobilized mouse hindlimb muscles during and after ischemia using high-field  $^{31}\text{P}$  MRS.

## METHODS

### Experimental model of cast immobilization

**Animals.** Young adult C57BL6 female mice (age 19–21 weeks; body weight 22–25 g) were studied. The animals were housed in an AALAC-accredited animal facility in a temperature ( $22 \pm 1^\circ\text{C}$ ), humidity ( $50 \pm 10\%$ ) and light controlled room (12 h light/dark cycles). The mice were acclimatized in the animal facility for a week before the start of the experiment. They were provided with water *ad libitum*, and food intake was monitored.

Non-invasive  $^{31}\text{P}$  ( $n = 8$ ) and  $^1\text{H}$  ( $n = 8$ ) MRS measurements were performed on the mouse gastrocnemius muscle before and after 2 weeks of immobilization. Biochemical data were acquired in mice immobilized for 2 weeks and in age-matched control healthy mice [ATP in eight animals (16 hindlimbs per group); total creatine (TCr) in three animals (six hindlimbs per group)]. All experimental procedures were approved by the Institutional Animal Care and Use Committee at the University of Florida.

### Casting procedure

Mice were anesthetized with gaseous isoflurane (3% induction, 0.5–2.5% maintenance), and the hindlimbs were immobilized as described previously (19). In brief, both hindlimbs were immobilized with the hip and knee joints fixed at  $\sim 160^\circ$  and  $\sim 180^\circ$ , respectively, and the ankle fixed at  $\sim 25$ – $30^\circ$  of plantar flexion, so that the

gastrocnemius muscle remained in a shortened position. The cast consisted of plaster of paris and encompassed both limbs and the caudal quarter of the body (cranial to the wings of the ileum). A very thin layer of padding was placed underneath the plaster of paris to prevent abrasions. The mice were monitored daily for chewed plaster, abrasions, venous occlusion, and potential problems with mobility.

### $^{31}\text{P}$ MRS

Spectra were acquired using a 11.1 T/470 MHz 40 cm horizontal bore Bruker Avance spectrometer (Paravision; V3.0.1) with 12 cm gradients (22 gauss/cm; rise time 170  $\mu\text{s}$ ) and a custom-built single-tuned 6 mm  $\times$  12 mm oblong  $^{31}\text{P}$  (190.5 MHz) surface coil. Mice were anesthetized using gaseous isoflurane (induction 3%; maintenance 0.5–1.5%). The right hindlimb was placed in an extended position. The  $^{31}\text{P}$  surface coil was centered over the right gastrocnemius muscle. Phantom studies revealed that, owing to the shallow depth profile of the coil,  $^{31}\text{P}$  spectra were primarily acquired from the gastrocnemius muscle *in vivo*. A 3-cm single-tuned  $^1\text{H}$  surface coil was placed underneath the hindlimb to provide anatomical information and localized magnetic field optimization. Typical line widths were  $\sim 45$  Hz. An inflatable blood pressure cuff (Harvard; inner diameter 1.5 cm) was placed around the animal's thigh.

A reversible ischemia model (30 min) was used to study kinetic changes in the energy-rich phosphate content and  $\text{pH}_i$  (20). On the basis of a pilot study, the ischemic period was set at 30 min to induce  $\sim 50\%$  depletion in the phosphocreatine (PCr) content and minimal change in  $\text{pH}_i$  ( $\text{pH}_i > 6.9$ ). Spectra were acquired with a 50  $\mu\text{s}$  square pulse, a pulse repetition time ( $TR$ ) of 2 s, sweep width of 10,000 Hz, and 8,000 complex data points. To determine the resting phosphate content, spectra at rest were acquired and signal-averaged over a 10 min period. Subsequently, sequential  $^{31}\text{P}$  spectra were collected in 30 s bins at rest (10 min), during ischemia (30 min), and throughout the recovery period after the release of the cuff (30 min).

**$^{31}\text{P}$  spectral and data analysis.** The spectra were manually phased, and the areas of the  $\gamma$ -ATP,  $\text{P}_i$ , and PCr peaks were determined using area integration (Xwin; Bruker, Billerica, MA, USA). Absolute concentrations of PCr and  $\text{P}_i$  are expressed as  $\text{mmol L}^{-1}$  intracellular water and were calculated from the PCr/ATP and  $\text{P}_i$ /ATP ratios and the biochemically determined ATP concentration after correction for  $T_1$  saturation.  $\text{pH}_i$  was calculated from the chemical shift of  $\text{P}_i$ , based on the equation  $\text{pH} = 6.75 + \log [(\delta - 3.27)/(5.69 - \delta)]$ , where  $\delta$  is the chemical shift of  $\text{P}_i$  in parts per million (ppm) relative to PCr. Free cytosolic [ADP] was calculated using the

creatine kinase equilibrium as described previously (16) for skeletal muscle, using an equilibrium constant of  $1.66 \times 10^9$  M (21) and a free Mg<sup>2+</sup> concentration of 1 mM (22). The free creatine concentration was calculated by subtracting the <sup>31</sup>P MRS-determined PCr concentration from the TCr content (determined by two independent methods: a colorimetric assay of extracted tissue and *in vivo* <sup>1</sup>H MRS). Intracellular Mg<sup>2+</sup> concentration was taken to be the same in both pre-immobilized and immobilized muscles, as no significant difference was detected in the Mg<sup>2+</sup>-dependent chemical shift of the β-ATP peak with immobilization. The cytosolic phosphorylation potential was calculated in its reciprocal form as [ADP][P<sub>i</sub>]/[ATP]. The predicted contribution of P<sub>i</sub> to the total muscle buffering capacity was calculated on the basis of its concentration (millimolar), pK<sub>a</sub>, and pH<sub>i</sub> as described previously (23,24).

Finally, dynamic changes in PCr concentrations were measured using complex principal component analysis (25). Kinetic changes in PCr during recovery were fitted to a single exponential curve using a non-linear curve-fitting algorithm, and the pseudo-first-order rate constant ( $k_{\text{PCr}}$ ) was determined (26).

The initial rate of PCr resynthesis ( $V_{\text{meas}}$ ; mM min<sup>-1</sup>), starting from the PCr concentration reached at the end of the ischemic period, was also determined, as a measure of the oxidative flux in muscle at the onset of recovery (26,27).  $V_{\text{meas}}$  was determined from the initial three data points in the recovery.  $V_{\text{meas}}$  was also used to calculate the apparent mitochondrial capacity,  $Q_{\text{max}}$ , based on the hyperbolic relationship between the  $V_{\text{meas}}$  and the phosphorylation ratio:

$$Q_{\text{max}} = V_{\text{meas}}(1 + K_m/[\text{ADP}][\text{P}_i]/[\text{ATP}]) \text{ mM min}^{-1} \quad (1)$$

where  $K_m = 0.11$  mM.

## <sup>1</sup>H MRS

Localized <sup>1</sup>H spectroscopy was performed at 11.1 T using a custom-built single-tuned <sup>1</sup>H loop gap coil (inner diameter = 1.4 cm, 470 MHz) and PRESS ( $TE = 60$  ms,  $TR = 6$  s, spectral width = 8,000 Hz, and averages = 300 scans). The typical voxel size was approximately  $2.8 \times 2.4 \times 1.27$  mm<sup>3</sup> and was centered in the gastrocnemius muscle (see Fig. 3). The localization of this voxel was guided by gradient-echo images acquired in three oblique, perpendicular directions ( $TE = 5$  ms,  $TR = 200$  ms, slice thickness 0.5 mm, matrix size  $256 \times 256$ , 12 slices). Localized shimming on this voxel was performed until a maximum line width of less than 30 Hz or 0.063 ppm was obtained.

<sup>1</sup>H-MRS data were processed with the AMARES algorithm using the MR user interface (jMRUI) 97.1 (28). The spectra obtained were apodized with a 5 Hz

Lorentzian function, and a zero-order and first-order phase correction were applied. The residual water signal was removed off-line using HLSVD pre-filtering (29). The creatine peak at a chemical shift of 3.02 ppm was fitted assuming a Gaussian line shape model function. The TCr concentration was quantified from the relaxation-corrected ratio of the fitted areas of the creatine peak to the water peak of the corresponding spectrum, using a previously validated method (30). The  $T_1$  and  $T_2$  relaxation times used for signal correction were measured to be  $1.85 \pm 0.10$  s and  $66.37 \pm 6.03$  ms, respectively ( $n = 5$ ) for creatine methyl protons, and  $1.45 \pm 0.05$  s and  $21.63 \pm 0.51$  ms ( $n = 5$ ) for water proton spins at 11.1 T. During immobilization, we did not detect any significant difference in the  $T_2$  relaxation for water ( $20.65 \pm 0.42$  ms). The concentration of water was assumed to be equal to  $42.4 \text{ mol (kg wet weight)}^{-1}$  (30,31). This concentration was used for both the pre-immobilized and post-immobilized muscle as we did not detect a significant difference in the wet to dry weight ratio of control ( $n = 6$ ;  $3.21 \pm 0.47$ ) and immobilized ( $n = 6$ ;  $3.17 \pm 0.42$ ) muscles or proton  $T_2$ .

## Biochemical analysis of muscle

At the end of the experiment, mice were euthanized by cervical dislocation, and gastrocnemius muscles were excised, snap-frozen, and stored at  $-80^\circ\text{C}$  for subsequent biochemical quantification of ATP and TCr. ATP concentrations were determined as described previously (32). Briefly, tissues (100 mg) were homogenized with a variable high-speed electric homogenizer (Power Gen 125; Fisher Scientific, Pittsburgh, PA, USA) after the sample had been placed in a vortex tube filled with 0.9% perchloric acid (5 volume/weight). After homogenization, the sample was centrifuged at  $4^\circ\text{C}$  (2,500G) for 15 min. The supernatant was extracted and added to 4 M KOH (1.125 v/w), and the sample was centrifuged at  $4^\circ\text{C}$  for 5 min. ATP was determined in the extracted supernatant using an ATP bioluminescence assay kit (Sigma).

To measure TCr, muscle samples stored at  $-80^\circ\text{C}$  were prepared for biochemical analysis by powdering the tissue under liquid N<sub>2</sub> and deproteinization in 0.5 M perchloric acid/1 mM EDTA (1.0 ml per 50 mg tissue). The supernatant was then neutralized with 2.1 M KHCO<sub>3</sub>/0.3 M MOPS (0.1 ml per 0.5 ml supernatant). The final supernatant was stored at  $-80^\circ\text{C}$  until analyzed. Muscle TCr content was measured by a non-enzymatic spectrophotometric assay described by De Saedeleer and Marechal (33).

TCr and ATP concentrations were determined in mmol (g wet weight)<sup>-1</sup> and mmol (L tissue)<sup>-1</sup>, assuming a muscle density of  $1.06 \text{ g mL}^{-1}$  (34). These were converted into mmol L<sup>-1</sup> intracellular water assuming a cellular water fraction of 0.73 (31,35).

## Data analysis

All statistical analyses were performed with SPSS for Windows, Version 11.0.1. Results are expressed as mean  $\pm$  SEM. Student's *t*-tests were used to compare data before immobilization and at 2 weeks of immobilization. Research hypotheses were tested at an  $\alpha$  level of 0.05.

## RESULTS

### Muscle energetics at rest

Representative  $^{31}\text{P}$  spectra acquired at rest from the mouse gastrocnemius muscle before and after 2 weeks of immobilization are shown in Fig. 1, and data are summarized in Table 1. After immobilization, resting  $\text{P}_i$  content (75%) and  $\text{P}_i/\text{PCr}$  (80%) were significantly increased compared with before ( $p < 0.001$ ; Fig. 2). In contrast, we did not observe a significant change in the

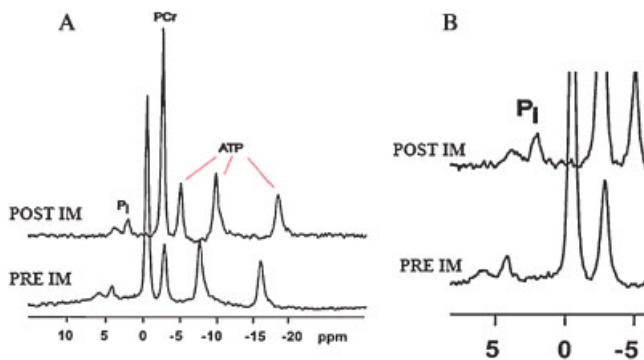


**Figure 1.**  $^{31}\text{P}$  MRS resting spectra from C57BL6 mouse gastrocnemius muscle. Data were acquired from the gastrocnemius muscle of a representative C57BL6 mouse before immobilization (PRE IM) and after 2 weeks of immobilization (POST IM). Note that the spectra illustrated in (B) allow better visualization of the  $\text{P}_i$  peak.

resting PCr content ( $p = 0.21$ ) or  $\text{pH}_i$  ( $p = 0.14$ ).  $^1\text{H}$  MRS data also showed that there was no significant change in resting [TCr] with immobilization, which was confirmed using biochemical analysis (Table 1). [ADP] and [ADP][ $\text{P}_i$ ]/[ATP] at rest were calculated on the basis of the creatine kinase equilibrium constant and showed no significant difference before and after immobilization. The absence of a difference in TCr content after immobilization was confirmed using biochemical analysis of extracted tissue (see below).

### Muscle energetics during ischemia and recovery

Dynamic changes in  $^{31}\text{P}$ -MRS spectra and the relative changes in [PCr],  $\text{P}_i/\text{PCr}$  ratio, and  $\text{pH}_i$  in the mouse gastrocnemius muscle during ischemia and the subsequent recovery period are shown in Figs. 4–6. During ischemia, there was a rapid decrease in [PCr], such that at the end of ischemia, PCr concentrations in pre-immobilized and immobilized muscles were approximately equal to 50% of their resting values ( $54 \pm 2\%$  vs  $52 \pm 6\%$ ). The rate of PCr depletion was similar in both pre-immobilized and immobilized muscles ( $0.55 \pm 0.01$  vs  $0.52 \pm 0.03 \text{ mM min}^{-1}$ ;  $p = 0.78$ ).

As expected, the decrease in [PCr] during ischemia was accompanied by a corresponding increase in [ $\text{P}_i$ ],  $\text{P}_i/\text{PCr}$  (Fig. 6A) and [ADP]. Despite different resting  $\text{P}_i$  concentrations, there were no detectable differences in the rates of  $\text{P}_i$  increase with immobilization ( $0.0376 \pm 0.006 \text{ mM min}^{-1}$  vs  $0.0334 \pm 0.11 \text{ mM min}^{-1}$  before and after immobilization, respectively). At the end of ischemia, the  $\text{P}_i$  content was increased to  $321 \pm 28\%$  and  $297 \pm 39\%$  of resting values in pre-immobilized and immobilized muscles, respectively (Table 1). However, because of large differences in the initial resting [ $\text{P}_i$ ] in immobilized muscles, end ischemia  $\text{P}_i$  concentrations were significantly different in the two groups. As an additional consequence, immobilized muscles showed a significantly

**Table 1.** Resting metabolite content and  $\text{pH}_i$  at rest and at the end of ischemia in C57BL6 mice ( $n = 8$ ) before immobilization (PRE IM) and 2 weeks after immobilization (POST IM)

	Rest		End of ischemia	
	PRE IM	POST IM	PRE IM	POST IM
[ $\text{P}_i$ ](mM)	$2.64 \pm 0.31$	$4.64 \pm 0.41^a$	$7.92 \pm 1.45$	$11.31 \pm 2.02^a$
[PCr] (mM)	$34.68 \pm 1.29$	$32.62 \pm 1.05$	$18.67 \pm 0.62$	$15.02 \pm 0.79^a$
TCr (mM)	$44.22 \pm 2.21$	$42.1 \pm 2.88$	—	—
$\text{P}_i/\text{PCr}$	$0.08 \pm 0.01$	$0.14 \pm 0.01^a$	$0.42 \pm 0.14$	$0.75 \pm 0.13^a$
$\text{pH}_i$	$7.19 \pm 0.02$	$7.17 \pm 0.02$	$7.12 \pm 0.02$	$7.05 \pm 0.06$
ADP ( $\mu\text{M}$ )	$31.97 \pm 4.75$	$26.43 \pm 3.4$	$124.7 \pm 6$	$143.9 \pm 9.7$
[ADP][ $\text{P}_i$ ]/[ATP] ( $\mu\text{M} \times$ )	$7.5 \pm 1.8$	$10.5 \pm 1.8$	$76.9 \pm 9.7$	$137.2 \pm 23.3^a$

Values are mean  $\pm$  SEM, obtained from MRS measurements.

<sup>a</sup>Significantly different from PRE IM ( $p < 0.05$ ).

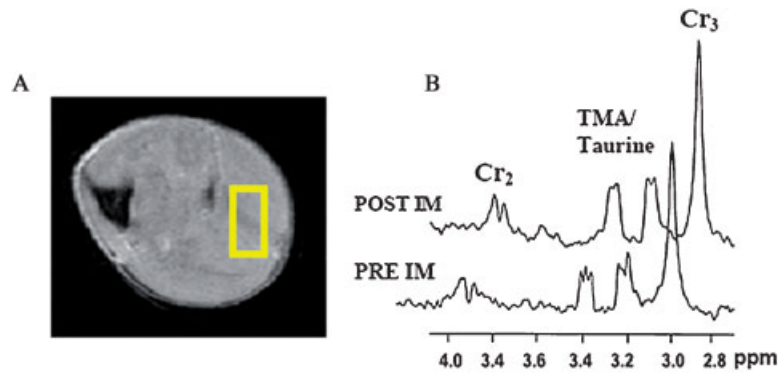


**Figure 2.** Resting  $P_i$  concentration and  $P_i/PCr$  ratio. Data were acquired from the gastrocnemius muscle of C57BL6 mice ( $n=8$ ) before immobilization (PRE IM) and after 2 weeks of immobilization (POST IM). Values are mean  $\pm$  SEM. \*Significantly different from PRE IM ( $p < 0.05$ ).

higher phosphorylation potential  $[ADP][P_i]/[ATP]$  at the end of ischemia (Table 1).

Changes in  $pH_i$  during ischemia were not significantly different in pre-immobilized and immobilized muscles  $[\Delta pH_i/\Delta PCr, 5.15 (\pm 0.85) \times 10^{-3}$  vs  $7.02 (\pm 1.5) \times 10^{-3}$  pH units  $mM^{-1}$ ; Fig. 6B] despite a difference in buffering capacity. At the end of ischemia, the apparent buffering capacity due to  $P_i$  was significantly increased in immobilized muscles ( $6.18 \pm 0.57$  slykes) compared with pre-immobilized muscles ( $3.38 \pm 0.54$  slykes). Neither group experienced intracellular acidosis, which might be expected to influence the rate of PCr recovery

kinetics (Table 1). Also, there was no significant change in  $[ATP]$  throughout the experiment.

The recovery kinetics of PCr, a well-established measure of overall mitochondrial function *in vivo*, is shown in Fig. 5B. Immobilization induced a significant reduction in  $k_{PCr}$  and the initial rate of PCr resynthesis ( $V_{meas}$ ), reflected in a significant decrease in measures of the *in vivo* mitochondrial function (Table 2). Furthermore, despite a significantly increased driving force (phosphorylation potential) at the end of ischemia, the apparent mitochondrial capacity,  $Q_{max}$ , was  $\sim 44\%$  lower in immobilized muscles than pre-immobilized muscles.

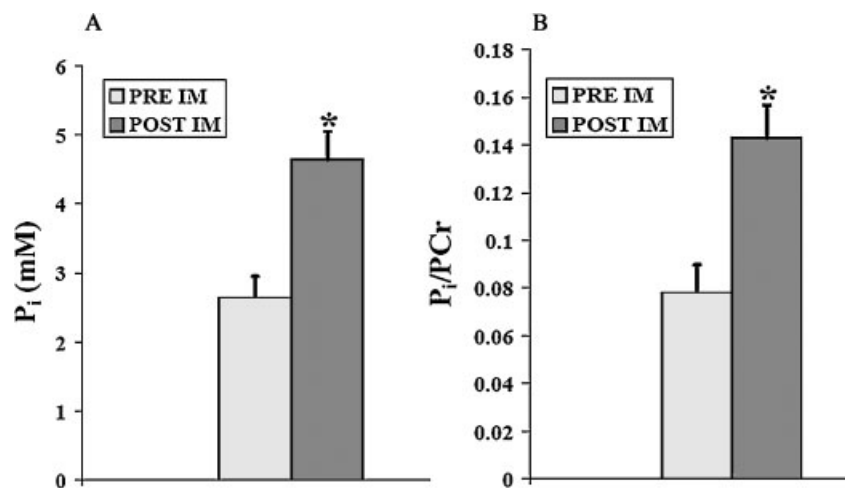


**Figure 3.**  $^1H$  MRS resting spectra from C57BL6 mouse gastrocnemius muscle. (A) A gradient-echo image obtained of the hindlimb of a mouse in the axial direction ( $TE = 5$  ms,  $TR = 200$  ms, slice thickness  $0.5$  mm,  $256 \times 128$  pixels<sup>2</sup>, 12 slices per direction). The box indicates the voxel ( $2.8 \times 1.2 \times 2.4$  mm<sup>3</sup>) selected for subsequent  $^1H$  MRS data collection. (B) Water unsuppressed  $^1H$  MRS PRESS spectra from the voxel shown in (A) ( $TE = 64$  ms,  $TR = 6000$  ms, 300 averages) before (PRE IM) and after (POST IM) immobilization. The spectra show signals for the methyl group of creatine ( $Cr_3$ ), the methylene group of creatine ( $Cr_2$ ), and the trimethyl ammonium (TMA)/taurine resonances.

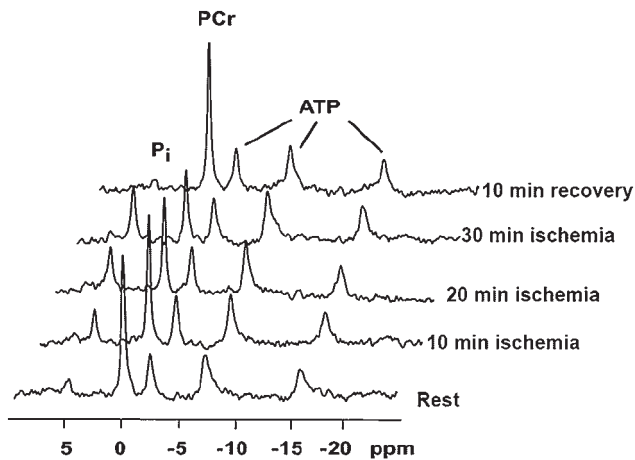


**Figure 4.**  $^{31}\text{P}$  spectra during ischemia and recovery. Representative  $^{31}\text{P}$  spectra obtained from the gastrocnemius muscle of C57BL6 mice at rest, after 10, 20, 30 min of ischemia, and after 10 min of recovery.

During recovery, there was a gradual decrease in  $\text{P}_i$  concentrations such that they returned to resting values within 6.5 min of recovery in both pre-immobilized and immobilized muscles. After 30 min of recovery,  $[\text{P}_i]$  in both muscle groups was lower than the resting value.

### Biochemical analysis

Biochemical analysis showed that immobilization did not induce a significant change in the resting concentrations of ATP [control vs immobilized:  $7.8 \pm 0.21$  vs  $7.8 \pm 0.16 \mu\text{mol} (\text{g wet weight})^{-1}$ ], TCr (control vs

immobilized:  $39.41 \pm 2.68$  vs  $42.7 \pm 1.67 \text{ mM}$ ), or free ADP (control vs immobilized:  $21.4 \pm 3.72$  vs  $28.54 \pm 3.42 \mu\text{M}$ ) or  $[\text{ADP}][\text{P}_i]/[\text{ATP}]$  (control vs immobilized:  $5.72 \pm 1.38$  vs  $9.76 \pm 0.09 \mu\text{M}$ ).

### DISCUSSION

Muscle disuse is a common phenomenon that induces a wide array of adaptations in skeletal muscle, which may negatively affect its function. The cast immobilization procedure used in this study is a clinically applicable model that induces significant muscle atrophy and loss of muscle strength in mouse hind-limb muscles (19). Importantly, this model allows examination of the effect of cast immobilization on skeletal muscle with fewer confounding factors than expected in a patient population. The primary purpose of the study was to determine the effect of cast immobilization, independent of injury or surgery, on the resting  $\text{P}_i$  content of mouse skeletal muscle.

Our results show that, after 2 weeks of cast immobilization, resting  $\text{P}_i$  content (75%) and  $\text{P}_i/\text{PCr}$  (80%) of the mouse gastrocnemius muscle are significantly increased compared with control, non-immobilized muscles. As all post-immobilization measures were performed before reloading, these data provide strong evidence that the increase in resting  $\text{P}_i$  content of skeletal muscle is the result of disuse and not injury, surgery or reloading-induced muscle damage.

The increase in  $\text{P}_i$  content with disuse may have important functional consequences. Disuse or inactivity has been associated with decreases in muscle cross-

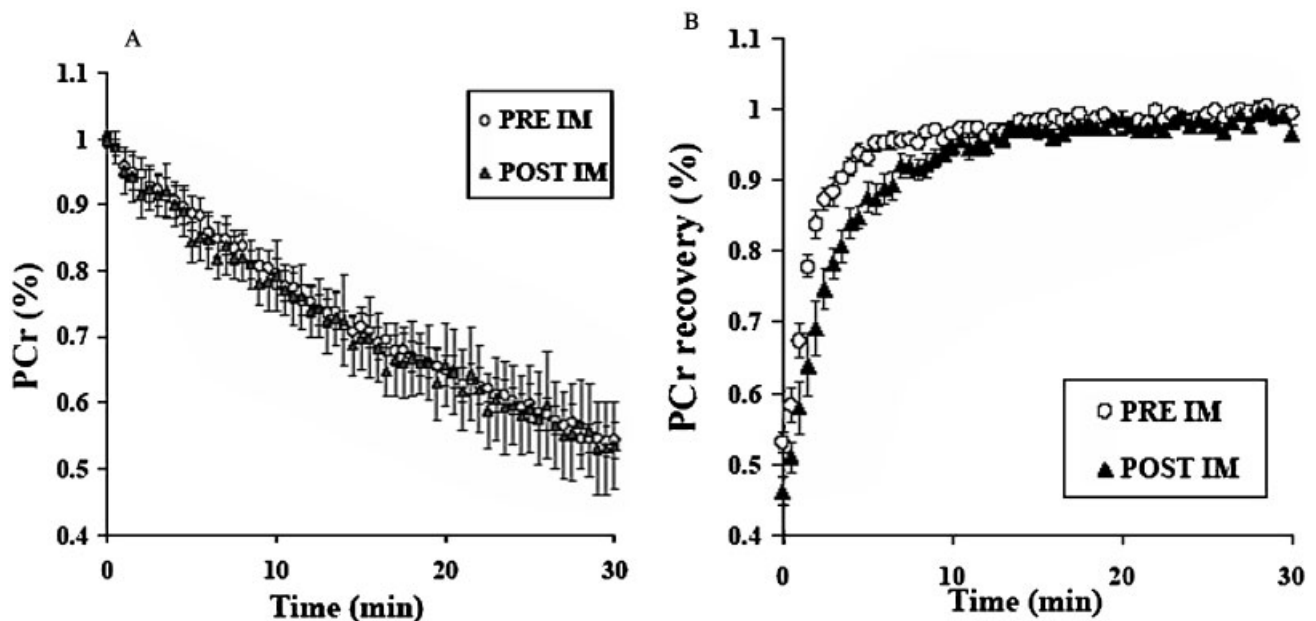


**Figure 5.**  $[\text{PCr}]$  during ischemia and recovery.  $\text{PCr}$  kinetics in the gastrocnemius muscle of C57BL6 mice ( $n=8$ ) during ischemia and subsequent recovery before immobilization (PRE IM) and after 2 weeks of immobilization (POST IM). (A) Changes in  $[\text{PCr}]$  during ischemia (30 min). (B) Changes in  $[\text{PCr}]$  during recovery (30 min) after ischemia. Values are means  $\pm$  SEM.

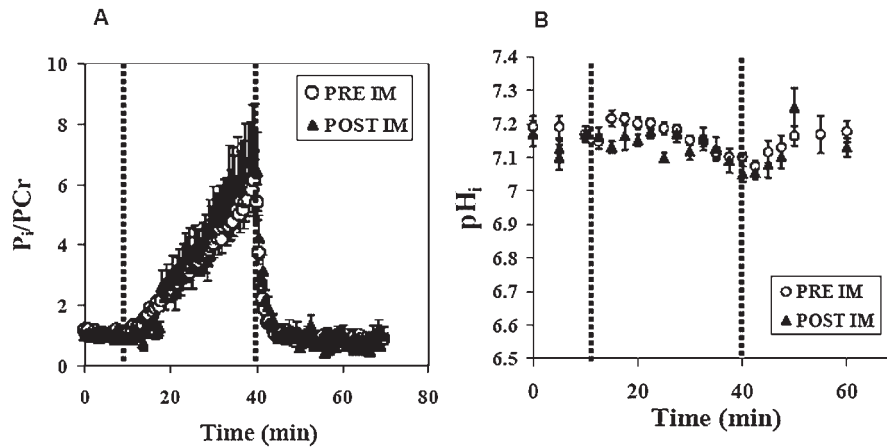


**Figure 6.**  $P_i/PCr$  and  $pH_i$  during ischemia and recovery.  $P_i/PCr$  (A) and  $pH_i$  (B) at rest and during ischemia and recovery. Time courses of changes from a representative C57BL6 mouse hindlimb before immobilization (PRE IM) and after immobilization (POST IM). Dotted lines indicate the start of the ischemia and recovery periods.

sectional area, strength and muscle-specific force (force/cross-sectional area) (2,3). The decrease in muscle-specific force has in part been linked to neural adaptations (4), but alterations in resting  $P_i$  content may also contribute (8). Using localized MRS, we observed a 64% increase in resting  $P_i$  content of the plantar flexors of patients with an ankle fracture after 6 weeks of lower limb immobilization (7,8). This returned to control values during the course of 10 weeks of rehabilitation, and a significant correlation was noted between  $[P_i]$  and specific plantar flexor torque. Numerous force mechanics studies in skinned, mammalian, skeletal muscle fibers have shown that an increase in intracellular  $[P_i]$  decreases isometric tension by inhibiting cross-bridge cycling and inducing a shift in the myofibrillar  $Ca^{2+}$  sensitivity (9–11,36). We recently showed in permeabilized single human muscle fibers that varying  $P_i$  concentrations within the ranges observed across immobilized individuals *in vivo* (4–10 mM) may vary force production by ~16% (8). Single-fiber force mechanics in type I human muscle fibers further revealed a non-linear relationship between relative force and  $P_i$  concentrations, with a  $F_{50}$  value (concentration of  $P_i$  that produces 50% isometric tension) of ~16 mM. (8). *In vitro* force mechanics measurements performed in other mammalian (rabbit psoas) muscle fibers have reported a  $k_i$  in the range 3–12 mM (37–39).

A large number of energetic studies have shown that transient changes in  $P_i$  concentrations also serve as an important  $pH_i$  buffer and help to regulate mitochondrial function (12–16). We examined the effect of alterations in resting  $P_i$  content with cast immobilization on regulators of mitochondrial phosphorylation (i.e.  $[ADP][P_i]/[ATP]$ ) during ischemia and measured the *in vivo* mitochondrial ATP synthesis capacity of the mouse gastrocnemius muscle as assessed by the rate of PCr resynthesis. We found that despite similar rates of PCr depletion and  $P_i$  increases during ischemia, the cytosolic phosphorylation potential  $[ADP][P_i]/[ATP]$  at the end of ischemia was 80% higher in immobilized muscles than control muscles.  $[ADP][P_i]/[ATP]$  was calculated on the basis of the creatine kinase equilibrium constant, in which the ATP concentration was determined biochemically. The total creatine concentration was measured using  $^1H$ -MRS and confirmed biochemically.

Despite a higher phosphorylation potential in the immobilized muscles at the end of ischemia, the rate of PCr resynthesis was significantly reduced in immobilized compared with control muscles. PCr recovery assessed by  $^{31}P$ -MRS has provided a valuable and sensitive evaluation of the *in vivo* oxidative capacity of skeletal muscle (18). The initial rate of PCr resynthesis provides an estimate of the rate of oxidative ATP synthesis or the oxidative flux at the onset of recovery (24,40) because of its relationship to

**Table 2.** PCr recovery rates and indices of oxidative capacity in C57BL6 mice ( $n = 8$ ) before (PRE IM) and 2 weeks after (POST IM) immobilization

	PRE IM	POST IM	Relative change (%)
$k_{PCr}$ ( $\text{min}^{-1}$ )	$0.43 \pm 0.04$	$0.31 \pm 0.038^a$	29
$V_{meas}$ ( $\text{mM min}^{-1}$ )	$6.58 \pm 0.46$	$4.63 \pm 0.42^a$	30
$Q_{max}$ ( $\text{mM min}^{-1}$ )	$17.58 \pm 1.47$	$9.76 \pm 0.72^a$	44

Values are mean  $\pm$  SEM, obtained from  $^1H$  NMR measurements of  $[TCr]$ .

$k_{PCr}$ , PCr recovery rate constant;  $V_{meas}$ , initial PCr resynthesis measured during first 2 min of recovery;  $Q_{max}$  based on  $V_{meas}$  and  $[ADP][P_i]/[ATP]$ .

<sup>a</sup>Significantly different from PRE IM ( $p < 0.05$ ).

its driving force  $[ADP][P_i]/[ATP]$  (41), as demonstrated during both *in vivo* (42) and *in vitro* (13,14) experiments of mitochondrial control. Thus,  $[ADP][P_i]/[ATP]$  at the onset of recovery and the initial PCr resynthesis rate can be used to calculate the maximum *in vivo* oxidative ATP synthesis rate ( $Q_{max}$ ), which reflects both the intrinsic mitochondrial capacity and the delivery of oxygen (43). The finding of a reduction in the indices of PCr recovery synthesis ( $k_{PCr}$ :  $0.43 \pm 0.04$  in immobilized muscle versus  $0.31 \pm 0.04$  in control) as well as the  $Q_{max}$  in the present study suggests that mitochondrial ATP production is significantly impaired in immobilized muscles. Our findings in immobilized mice hindlimb muscles confirm and extend other *in vivo* observations made in human (44) and rat (45) muscles. *In vitro* studies report decreases in oxidative capacity ranging between 13% and 50% depending on the duration of immobilization, the oxidative enzymes studied, and the muscle of interest (46–48). As *in vivo* MRS assays the metabolic capacity of the whole muscle, rather than individual fibers, the reduction in oxidative capacity reported in this study is probably the result of true alterations in mitochondrial function and a shift in fiber type composition. A large number of studies have shown a decrease in the proportion of type I fibers (slow oxidative) and concomitant increase in type II (fast glycolytic) fibers in disused muscles (49,50).

Our study also suggests that an increase in the resting  $P_i$  content may enhance the buffering capacity of skeletal muscle to aid  $pH_i$  regulation.  $pH_i$  of skeletal muscle is the result of a number of processes: glycogenolytic proton production (34), passive buffering of protons, net PCr hydrolysis, and proton extrusion from the cell (35). The buffering systems in ischemic skeletal muscle consist of intrinsic buffering by proteins, bicarbonate, and  $P_i$  (16,43). The contribution of  $P_i$  to total muscle buffering can be estimated from its  $pK_a$  and concentration and  $pH_i$  (16,43). In this study, we found that the apparent buffering capacity due to  $P_i$  in immobilized muscles was ~82% higher than in pre-immobilized muscles. The predicted contribution of  $P_i$  to the total muscle buffering capacity was  $6.18 \pm 0.57$  slykes in pre-immobilized muscles and  $3.38 \pm 0.54$  slykes in control muscles. These findings suggest that after immobilization there may be an added benefit to the raised basal  $P_i$  in that it enhances the buffering capacity of skeletal muscles, allowing increased anaerobic ATP production while minimizing intracellular acidosis.

The pathophysiological mechanism responsible for inducing an increase in resting  $P_i$  content with disuse is not clear. In our initial observation, we speculated that the increase in resting  $P_i$  content may be due to muscle damage. A high  $P_i$ /PCr ratio is a well-established non-specific marker of muscular damage and is well documented in exercise-induced injury as well as neuromuscular diseases (51). However, Frimel *et al.* (52) used a combination of  $T_2$ -weighted imaging and

histological markers of muscle damage and did not detect muscle damage or macrophage infiltration in the mouse gastrocnemius muscle after 2 weeks of immobilization. In addition, as all MR measurements were performed at the end of immobilization, before reloading, the increase in resting  $P_i$  content is not the result of reloading injury. It is also very unlikely that the increase in  $P_i$  content after cast immobilization is due to a fiber type shift from slow to fast, as type II fibers have a lower  $P_i$  content than type I fibers (53,54). Finally, we should point out that, despite the fact that we could not detect a significant decrease in the resting PCr concentration after immobilization, the sums of resting  $P_i$  and PCr concentration in the immobilized and pre-immobilized muscles were almost identical ( $37.00 \pm 1.22$  vs  $37.88 \pm 1.21$  mM).

To our knowledge, this is the first study to examine the effect of immobilization on the *in vivo* bioenergetics of peripheral skeletal muscle in mice. Muscle energetic studies in mice are challenging because of the small muscle volume and the need for high temporal resolution. In this study we were able to monitor the PCr recovery rate in the mouse gastrocnemius muscle with a temporal resolution of 30 s, using optimized surface coils and high magnetic field strength (470 MHz; 11.1 T). The PCr recovery time constant values from control muscles in the present work (PCr depletion, 46%;  $2.6 \pm 0.27$  min) are within the range of data reported previously from mouse hindlimb muscles using *in situ* tetanic contractions (PCr depleted by 52%;  $2.7 \pm 0.2$  min) (55).

The present results provide additional insight into the adaptations in skeletal muscle energy metabolism after a period of immobilization. In summary, our findings show that the increase in resting  $P_i$  content of skeletal muscle previously observed in patients during cast immobilization is not the result of surgery/injury or reloading-induced muscle damage and can also be observed in an animal model of cast immobilization.  $P_i$  has been shown to reduce muscle force, by inhibiting cross-bridge cycling and inducing a shift in the myofibrillar  $Ca^{2+}$  sensitivity. In addition, we found that the increase in resting  $P_i$  content has a significant effect on the cytosolic phosphorylation potential during transient ischemia and increases the buffer capacity of skeletal muscle. Despite an increased driving force, immobilized muscles showed a marked reduction in mitochondrial ATP-producing capacity.

## Acknowledgements

We sincerely thank Mike Hall and Gabriel Gaidosh for their contributions to this study. NMR data were obtained at the Advanced Magnetic Resonance Imaging and Spectroscopy (AMRIS) facility in the Evelyn F. and William L. McKnight Brain Institute of the University of Florida. J.S. was supported as a postdoctoral fellow by grant VA-B3461H.

## REFERENCES

- Hamilton MT, Booth FW. Skeletal muscle adaptation to exercise: a century of progress. *J Appl Physiol* 2000; **88**: 327–331.
- Adams GR, Hather BM, Dudley GA. Effect of short-term unweighting on human skeletal muscle strength and size. *Aviat Space Environ Med* 1994; **65**: 1116–1121.
- Berg HE, Larsson L, Tesch PA. Lower limb skeletal muscle function after 6 wk of bed rest. *J Appl Physiol* 1997; **82**: 182–188.
- McComas AJ. Human neuromuscular adaptations that accompany changes in activity. *Med Sci Sports Exerc* 1994; **26**: 1498–1509.
- Widrick JJ, Knuth ST, Norenberg KM, Romatowski JG, Bain JL, Riley DA, Karhanek M, Trappe SW, Trappe TA, Costill DL, Fitts RH. Effect of a 17 day spaceflight on contractile properties of human soleus muscle fibres. *J Physiol* 1999; **516**: 915–930.
- Pathare NC, Stevens JE, Walter GA, Shah P, Jayaraman A, Tillman SM, Scarborough MT, Parker Gibbs C, Vandeborne K. Deficit in human muscle strength with cast immobilization: contribution of inorganic phosphate. *Eur J Appl Physiol* 2006; **98**: 71–78.
- Vandeborne K, Elliott MA, Walter GA, Abdus S, Okereke E, Shaffer M, Tahernia D, Esterhai JL. Longitudinal study of skeletal muscle adaptations during immobilization and rehabilitation. *Muscle Nerve* 1998; **21**: 1006–1012.
- Pathare N, Walter GA, Stevens JE, Yang Z, Okerke E, Gibbs JD, Esterhai JL, Scarborough MT, Gibbs CP, Sweeney HL, Vandeborne K. Changes in inorganic phosphate and force production in human skeletal muscle after cast immobilization. *J Appl Physiol* 2005; **98**: 307–314.
- Dantzig JA, Goldman YE, Millar NC, Laktis J, Homsher E. Reversal of the cross-bridge force-generating transition by photo-generation of phosphate in rabbit psoas muscle fibres. *J Physiol* 1992; **451**: 247–278.
- Cooke R, Franks K, Luciani GB, Pate E. The inhibition of rabbit skeletal muscle contraction by hydrogen ions and phosphate. *J Physiol* 1988; **395**: 77–97.
- Kentish JC. The effects of inorganic phosphate and creatine phosphate on force production in skinned muscles from rat ventricle. *J Physiol* 1986; **370**: 585–604.
- Erecinska M, Wilson DF. On the mechanism of regulation of cellular respiration. The dependence of respiration on the cytosolic [ATP],[ADP] and [P<sub>i</sub>]. *Adv Exp Med Biol* 1977; **94**: 271–278.
- Holian A, Owen CS, Wilson DF. Control of respiration in isolated mitochondria: quantitative evaluation of the dependence of respiratory rates on [ATP], [ADP], and [P<sub>i</sub>]. *Arch Biochem Biophys* 1977; **181**(1): 164–171.
- Gyulai L, Roth Z, Leigh JS Jr, Chance B. Bioenergetic studies of mitochondrial oxidative phosphorylation using <sup>31</sup>P phosphorus NMR. *J Biol Chem* 1985; **260**: 3947–3954.
- Kemp GJ, Thompson CH, Sanderson AL, Radda GK. pH control in rat skeletal muscle during exercise, recovery from exercise, and acute respiratory acidosis. *Magn Reson Med* 1994; **31**: 103–109.
- Kemp GJ, Radda GK. Quantitative interpretation of bioenergetic data from <sup>31</sup>P and <sup>1</sup>H magnetic resonance spectroscopic studies of skeletal muscle: an analytical review. *Magn Reson Q* 1994; **10**: 43–63.
- Walter G, Vandeborne K, McCully KK, Leigh JS. Noninvasive measurement of phosphocreatine recovery kinetics in single human muscles. *Am J Physiol* 1997; **272**: C525–534.
- Radda GK, Gadian DG, Ross BD. Energy metabolism and cellular pH in normal and pathological conditions. A new look through <sup>31</sup>P phosphorus nuclear magnetic resonance. *Ciba Found Symp* 1982; **87**: 36–57.
- Frimel TN, Kapadia F, Gaidosh GS, Li Y, Walter GA, Vandeborne K. A model of muscle atrophy using cast immobilization in mice. *Muscle Nerve* 2005; **32**: 672–674.
- in 't Zandt HJ, Oerlemans F, Wieringa B, Heerschap A. Effects of ischemia on skeletal muscle energy metabolism in mice lacking creatine kinase monitored by *in vivo* <sup>31</sup>P nuclear magnetic resonance spectroscopy. *NMR Biomed* 1999; **12**: 327–334.
- Veech RL, Lawson JW, Cornell NW, Krebs HA. Cytosolic phosphorylation potential. *J Biol Chem* 1979; **254**: 6538–6547.
- Golding EM, Teague WE Jr, Dobson GP. Adjustment of K<sup>+</sup> to varying pH and pMg for the creatine kinase, adenylate kinase and ATP hydrolysis equilibria permitting quantitative bioenergetic assessment. *J Exp Biol* 1995; **198**: 1775–1782.
- Conley KE, Blei ML, Richards TL, Kushmerick MJ, Jubrias SA. Activation of glycolysis in human muscle *in vivo*. *Am J Physiol* 1997; **273**: C306–315.
- Kemp GJ, Thompson CH, Barnes PR, Radda GK. Comparisons of ATP turnover in human muscle during ischemic and aerobic exercise using <sup>31</sup>P magnetic resonance spectroscopy. *Magn Reson Med* 1994; **31**: 248–258.
- Elliott MA, Walter GA, Swift A, Vandeborne K, Schotland JC, Leigh JS. Spectral quantitation by principal component analysis using complex singular value decomposition. *Magn Reson Med* 1999; **41**: 450–455.
- Meyer RA. Linear dependence of muscle phosphocreatine kinetics on total creatine content. *Am J Physiol* 1989; **257**: C1149–1157.
- McCully KK, Vandeborne K, DeMeirleir K, Posner JD, Leigh JS Jr. Muscle metabolism in track athletes, using <sup>31</sup>P magnetic resonance spectroscopy. *Can J Physiol Pharmacol* 1992; **70**: 1353–1359.
- Vanhamme L, van den Boogaart A, Van Huffel S. Improved method for accurate and efficient quantification of MRS data with use of prior knowledge. *J Magn Reson* 1997; **129**: 35–43.
- de Beer R van Ormondt D. *In vivo* magnetic resonance spectroscopy I: probe heads and radio frequency pulses spectrum analysis. In *NMR*. Springer Verlag: New York, 1992; 201–258.
- Bottomley PA, Lee Y, Weiss RG. Total creatine in muscle: imaging and quantification with proton MR spectroscopy. *Radiology* 1997; **204**: 403–410.
- Forsberg AM, Nilsson E, Werneman J, Bergstrom J, Hultman E. Muscle composition in relation to age and sex. *Clin Sci (Lond)* 1991; **81**: 249–256.
- Jucker BM, Rennings AJ, Cline GW, Shulman GI. <sup>13</sup>C and <sup>31</sup>P NMR studies on the effects of increased plasma free fatty acids on intramuscular glucose metabolism in the awake rat. *J Biol Chem* 1997; **272**: 10464–10473.
- De Saedeleer M, Marechal G. Chemical energy usage during isometric twitches of frog sartorius muscle intoxicated with an isomer of creatine, beta-guanidinopropionate. *Pflugers Arch* 1984; **402**: 185–189.
- Mendez J, Keys A. Density and composition of mammalian muscle. *Metabolism* 1960; **9**: 184–188.
- Sjogaard G, Saltin B. Extra- and intracellular water spaces in muscles of man at rest and with dynamic exercise. *Am J Physiol* 1982; **243**: R271–280.
- Millar NC, Homsher E. Kinetics of force generation and phosphate release in skinned rabbit soleus muscle fibers. *Am J Physiol* 1992; **262**: C1239–1245.
- Wilson GJ, Shull SE, Cooke R. Inhibition of muscle force by vanadate. *Biophys J* 1995; **68**: 216–226.
- Tesi C, Colomo F, Nencini S, Piroddi N, Poggesi C. The effect of inorganic phosphate on force generation in single myofibrils from rabbit skeletal muscle. *Biophys J* 2000; **78**: 3081–3092.
- Cooke R, Pate E. The effects of ADP and phosphate on the contraction of muscle fibers. *Biophys J* 1985; **48**: 789–798.
- Boska M. Estimating the ATP cost of force production in the human gastrocnemius/soleus muscle group using <sup>31</sup>P MRS and <sup>1</sup>H MRI. *NMR Biomed* 1991; **4**: 173–181.
- Kemp GJ, Taylor DJ, Radda GK. Control of phosphocreatine resynthesis during recovery from exercise in human skeletal muscle. *NMR Biomed* 1993; **6**: 66–72.
- Kushmerick MJ, Meyer RA, Brown TR. Regulation of oxygen consumption in fast- and slow-twitch muscle. *Am J Physiol* 1992; **263**: C598–606.
- Kemp GJ, Taylor DJ, Thompson CH, Hands LJ, Rajagopalan B, Styles P, Radda GK. Quantitative analysis by <sup>31</sup>P magnetic resonance spectroscopy of abnormal mitochondrial oxidation in skeletal muscle during recovery from exercise. *NMR Biomed* 1993; **6**: 302–310.
- Kitahara A, Hamaoka T, Murase N, Homma T, Kurosawa Y, Ueda C, Nagasawa T, Ichimura S, Motobe M, Yashiro K, Nakano S, Katsumura T. Deterioration of muscle function after 21-day forearm immobilization. *Med Sci Sports Exerc* 2003; **35**: 1697–1702.

45. Yoshida N, Ikata T, Sairyo K, Matsuura T, Sasa T, Koga K, Fukunaga M. Evaluation of disuse atrophy of rat skeletal muscle based on muscle energy metabolism assessed by <sup>31</sup>P-MRS. *J Physiol Anthropol Appl Human Sci* 2001; **20**: 247–252.
46. Blakemore SJ, Rickhuss PK, Watt PW, Rennie MJ, Hundal HS. Effects of limb immobilization on cytochrome c oxidase activity and GLUT4 and GLUT5 protein expression in human skeletal muscle. *Clin Sci (Lond)* 1996; **91**: 591–599.
47. Jansson E, Sylven C, Arvidsson I, Eriksson E. Increase in myoglobin content and decrease in oxidative enzyme activities by leg muscle immobilization in man. *Acta Physiol Scand* 1988; **132**: 515–517.
48. Hikida RS, Gollnick PD, Dudley GA, Convertino VA, Buchanan P. Structural and metabolic characteristics of human skeletal muscle following 30 days of simulated microgravity. *Aviat Space Environ Med* 1989; **60**: 664–670.
49. Booth FW, Kelso JR. Cytochrome oxidase of skeletal muscle: adaptive response to chronic disuse. *Can J Physiol Pharmacol* 1973; **51**: 679–681.
50. Desplanches D, Mayet MH, Sempore B, Flandrois R. Structural and functional responses to prolonged hindlimb suspension in rat muscle. *J Appl Physiol* 1987; **63**: 558–563.
51. McCully KK, Kent JA, Chance B. Application of <sup>31</sup>P magnetic resonance spectroscopy to the study of athletic performance. *Sports Med* 1988; **5**: 312–321.
52. Frimel TN, Walter GA, Gibbs JD, Gaidosh GS, Vandeborne K. Noninvasive monitoring of muscle damage during reloading following limb disuse. *Muscle Nerve* 2005; **32**: 605–612.
53. Kushmerick MJ, Moerland TS, Wiseman RW. Mammalian skeletal muscle fibers distinguished by contents of phosphocreatine, ATP, and Pi. *Proc Natl Acad Sci USA* 1992; **89**: 7521–7525.
54. Vandeborne K, Walter G, Ploutz-Snyder L, Staron R, Fry A, De Meirleir K, Dudley GA, Leigh JS. Energy-rich phosphates in slow and fast human skeletal muscle. *Am J Physiol* 1995; **268**: C869–876.
55. Hancock CR, Brault JJ, Wiseman RW, Terjung RL, Meyer RA. <sup>31</sup>P-NMR observation of free ADP during fatiguing, repetitive contractions of murine skeletal muscle lacking AK1. *Am J Physiol Cell Physiol* 2005; **288**: C1298–C1304.